Collisionless Electron Heating in an Inductively Coupled Discharge

M. M. Turner*
School of Physical Sciences, Dublin City University, Glasnevin, Dublin 9, Ireland
(Received 28 June 1993)

We present self-consistent simulations and analysis of the electron heating processes in an inductively coupled discharge. The results show that collisionless electron heating is predominant at pressures of 10 mTorr or less. The collisionless excitation mechanism is a warm plasma effect, analogous to the anomalous skin effect in metals.

PACS numbers: 52.80.Pi, 52.50.−b, 52.65.+z, 52.75.−d

Babat [1] introduced the distinction between H discharges and E discharges. These are both types of high frequency or radio frequency (rf) discharges, but E discharges—or capacitively coupled discharges—are excited by a directly applied electrostatic field, whereas H discharges are sustained through an electromagnetic interaction between the plasma and a current flowing in a nearby antenna. H discharges are often referred to as inductively coupled. Capacitively coupled discharges have been widely discussed in recent years, particularly because of the occurrence of non-Ohmic electron heating [2]. Ohmic heating is effective only when the electron collision frequency ν is substantially larger than the angular driving frequency ω. However, an E discharge can be maintained by a collisionless interaction between electrons and the moving rf sheaths when $\nu/\omega \approx 1$ [3]. Recent demonstrations [4–6] that a dense inductively excited plasma can exist when $\nu/\omega \lesssim 0.1$ suggest that there is a powerful collisionless heating process in H discharges. This Letter shows definitively that there is such a mechanism. We begin by outlining a version of the accepted [7,8] theory of Ohmic excitation of H discharges. By comparing this theory with the results of a self-consistent kinetic simulation, we show that the collisional heating model is inadequate when $\nu/\omega \lesssim 1$. The collisionless heating that then occurs is described by the Vlasov-Maxwell kinetic theory [9,10]. Finally, we present simulation results for discharge parameters of practical interest, and hence show that the conditions for collisionless heating can be satisfied in experiments, particularly those of [4–6].

H discharges characteristically have a complicated geometry—the discharge usually either encloses or is enclosed by an inductive coil [7,8], which forms the rf antenna. Moreover, the presence of a voltage across the coil usually entails some residual capacitive coupling which may not be negligible in practice. We wish to discuss the field-plasma interaction without regard to these features, and we do this by adopting a one-dimensional model in which a plasma is enclosed between two infinite plane walls separated by a distance L along the x axis. Since both walls are held at ground potential, capacitive coupling is strictly eliminated from this configuration. We assume that the wall at $x = L$ reflects electromagnetic radiation, and we represent the inductive excitation by launching a plane electromagnetic wave into the plasma from the origin; any reflected radiation that returns to the origin is absorbed there. The wave is considered to be sourced from a linear current density flowing in the y-z plane. We fix the wave polarization by arbitrarily choosing the y direction for this current, hereafter denoted $\mathcal{J}_y$. Then the boundary condition for the fields at the origin is $H_z = \mathcal{J}_y$ and the equations to be satisfied within the plasma are

$$\frac{\partial E_y}{\partial x} = -i\omega B_z, \quad \frac{\partial H_z}{\partial x} = -J_y, \tag{1}$$

where J_y is the plasma current density and $B_z = \mu_0 H_z$. We assume that all these quantities have a harmonic time variation with angular frequency ω, and we take it that $\omega \ll \omega_p$, where ω_p is the plasma frequency, so that the displacement current term need not appear in Eq. (1). It is convenient to characterize the absorption of power by the plasma using the surface impedance $\zeta \equiv (E_y/H_z)_{x=0}$. We can write the time-averaged power absorbed by the plasma P in terms of the real part of ζ, denoted by ζ':

$$P = \frac{1}{2}\zeta' |H_z|^2 = \frac{1}{2}\zeta' |\mathcal{J}_y|^2. \tag{2}$$

If we assume that the plasma has uniform electron density n_e and conductivity $\sigma = n_e e^2/m_e(\nu + i\omega)$, where e and m_e are the electronic charge and mass, then by setting $J_y = \sigma E_y$ we can eliminate B_z, H_z, and J_y from Eq. (1) to form the ubiquitous [4,7,8,11] complex wave equation

$$\frac{d^2 E_y}{dy^2} - i\omega\mu_0\sigma E_y = 0. \tag{3}$$

With the approximations already mentioned this equation may be solved for E_y and B_z may then be found from one of the equations in (1). Hence the collisional surface impedance, ζ_c, can be shown to be

$$\zeta_c = \frac{i\omega\mu_0}{k}\tanh kL, \tag{4}$$

where

$$k \simeq \frac{w_p}{c}\left[\sqrt{\phi(1+\phi)/2} + i\sqrt{\phi(1-\phi)/2}\right] \tag{5}$$

0031-9007/93/71(12)/1844(4)$06.00

and $\phi = (1 + \nu^2/\omega^2)^{-1/2}$. The real part of the surface impedance predicted by Eq. (4) is shown in Fig. 1, as a function of ν. We next compare these analytical results with a simulation based on the particle in cell algorithm with Monte Carlo collisions (PIC-MCC) [12–14]. The essentials of this well-known technique as it has been applied to E discharges are described elsewhere [14]. We have added a numerical solution of the electromagnetic field equations for E_y and B_z using the Langdon-Dawson advective algorithm [12]. For comparison with Eq. (4) only the response of the electrons was considered; the ions were represented as a uniform neutralizing background charge. The plasma density was held constant by specularly reflecting electrons from the boundaries and a constant electron collision frequency was imposed. All collisions were assumed to be elastic. The geometry and orientation of the field components were as in the analytical model described above. This simulation entails all the assumptions leading to Eq. (4) except the cold plasma approximation. The results of the simulation are also shown in Fig. 1. It is clear that when $\nu \gtrsim \omega$ the simulation is in excellent agreement with Eq. (4). However, when $\nu \lesssim \omega$, the simulation data depart from the analytical result. As we show below, this signals the breakdown of Eq. (3) and the onset of collisionless heating.

The collisionless electron heating is a warm plasma effect. In a cold collisionless plasma each electron samples the electric field at a single location in space, and since the field has a harmonic time variation it averages to zero everywhere, so no energy can be gained. However, if the electrons are in thermal motion, they sample the field along some trajectory and in general the field does not average to zero along a trajectory. The field is confined to the skin depth layer, of width δ, so if an electron can traverse the skin depth layer in a time that is short

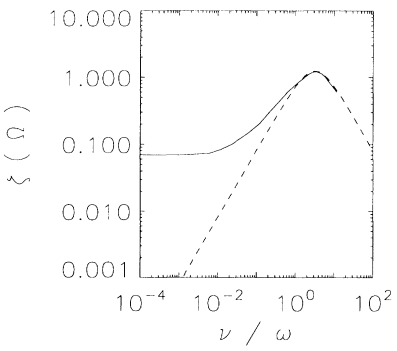

FIG. 1. The real part of the surface impedance ζ as a function of the ratio of the electron collision frequency ν to the angular excitation frequency ω. The solid curve shows the result of the simulation discussed in the text, while the dashed curve is the prediction of Eq. (4). Relevant plasma parameters are $L = 4$ cm, $n_e = 10^{11}$ cm^{-3}, $\omega = 2\pi \times 13.56$ MHz, and in the simulation $T_e = 5$ eV, in the low collision frequency limit.

compared to the period of the field, then it will gain net energy from the field. This situation arises when

$$\omega\,\delta \lesssim (k_B T_e/m_e)^{1/2}, \tag{6}$$

where T_e is the electron temperature and k_B is Boltzmann's constant. An immediate consequence of this nonnegligible thermal motion is that a field applied to one part of the plasma at some time can affect the current everywhere in the plasma at all later times, so we can no longer write $J_y = \sigma E_y$, but instead [9,10]

$$J_y(x,t) = \int dx' \int_{-\infty}^{t} dt'\ \Sigma(x - x', t - t') E_y(x', t'), \tag{7}$$

where $\Sigma(x,t)$ is some effective conductivity. We can avoid an explicit integration over time by the presumption of harmonic time variation, and so rewrite Eq. (3) as

$$\frac{d^2 E_y}{dx^2} - i\omega\mu_0 \int dx'\ \Sigma(x - x') E_y(x') = 0. \tag{8}$$

The distributed conductivity $\Sigma(x)$ is determined by suitably linearizing the Vlasov-Maxwell equations [9,10]. Assuming a Maxwellian electron velocity distribution, and making other approximations which are valid when condition (6) is satisfied, Eq. (8) can be solved for the case of a half-infinite plasma with a boundary at the origin that specularly reflects electrons [10]. The result for the surface impedance is

$$\zeta_a = \frac{2\mu_0\omega\delta_a}{3}\left(\frac{1}{\sqrt{3}} + i\right), \tag{9}$$

where δ_a is a skin depth, defined as

$$\delta_a = \left[\left(\frac{2k_B T_e}{\pi m_e}\right)^{1/2} \frac{c^2}{\omega_p^2 \omega}\right]^{1/3}. \tag{10}$$

The assumption that the plasma is half infinite is valid when

$$\delta_a \lesssim L. \tag{11}$$

This condition is not strongly satisfied under the circumstances of Fig. 1, and consequently the low pressure limit of the surface impedance shown is substantially smaller than the value predicted by Eq. (9). The surface impedance calculated from the simulation approaches the prediction of Eq. (9) to within a few percent when $\delta_a/L \lesssim 0.1$ as shown in Fig. 2.

The inequalities (6) and (11) imply interesting scaling relations. For a plasma of fixed size, density, and temperature, there is a finite range of frequencies that allows effective collisionless excitation. At excessively high frequency, electrons cannot traverse the skin depth in a rf period; then (6) is not satisfied. At excessively low frequency, the skin depth is larger than the plasma size and (11) is violated. Together, these conditions imply that, for a plasma of fixed size and temperature, there is a

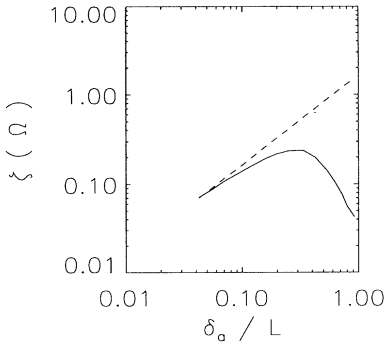

FIG. 2. The effect of finite plasma size on the real part of the collisionless surface impedance. The solid line shows the simulation result for a finite plasma of size L, while the dashed line is the prediction of Eq. (10) for half-infinite plasma with the same skin depth. The plasma density was varied between 10^9 and 10^{13} cm^{-3}, and the other parameters were as in Fig. 1.

threshold plasma density below which collisionless excitation is not possible at all. A slice through a part of the parameter space that exhibits this effect appears in Fig. 3. Equations (6) and (11) can be combined to show that the threshold density depends only on L and is

$$n_e^{(\text{threshold})} \approx \left(\frac{2}{\pi}\right)^{1/2} \frac{c^2 \varepsilon_0 m_e}{L^2 e^2}, \tag{12}$$

while the corresponding angular excitation frequency is

$$\omega^{(\text{threshold})} \approx \frac{1}{L}\left(\frac{k_B T_e}{m_e}\right)^{1/2}. \tag{13}$$

By fortuitous coincidence the frequencies required are near the standard 13.56 MHz, for common choices of L and reasonable values of T_e. We note that a minimum plasma density for effective inductive excitation has been

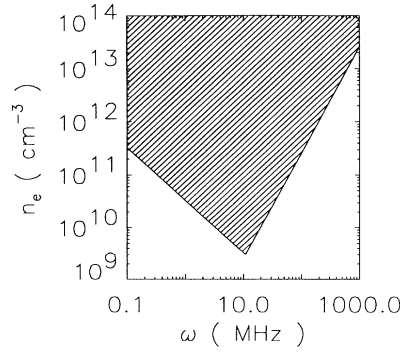

FIG. 3. A slice through the parameter space, showing a region where collisionless excitation is effective (shaded). Note the global minimum electron density for effective collisionless excitation. To the right of the minimum, condition (6) is the operative constraint; to the left, condition (11). Other parameters are $L = 4$ cm, $T_e = 5$ eV.

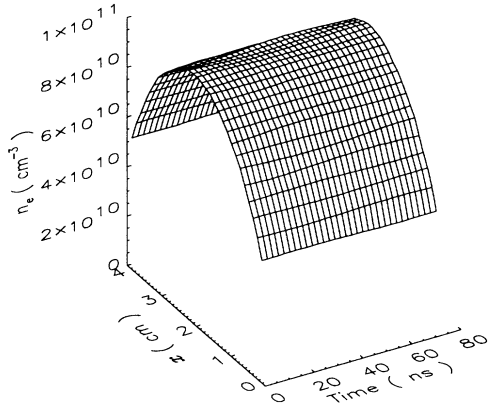

FIG. 4. The plasma electron density calculated by the simulation, as a function of time and position during a single rf cycle. The conditions were a pressure of 1 mTorr and a boundary current density $\mathcal{J}_y \simeq 600$ A m^{-1}. Note that the mesh density in this figure does not resolve the sheath regions, which have been omitted for clarity: the plasma density goes essentially to zero at the boundaries.

observed experimentally [5], although it is not clear that the effect is confined to low pressure (other explanations have been offered [8]).

We now present self-consistent simulations to show that the collisionless condition $\nu \lesssim \omega$ is satisfied in experiments under conditions of practical interest [4–6]. The simulation used cross sections for electron [15–17] and ion collisions [18] with argon. It was assumed that both electrons and ions were absorbed if they reached the boundaries, and no secondaries were emitted. In the usual way, we allowed the simulation to proceed for many rf periods until a harmonic steady state was attained. As in [19], we chose to reduce the ion mass so that convergence took

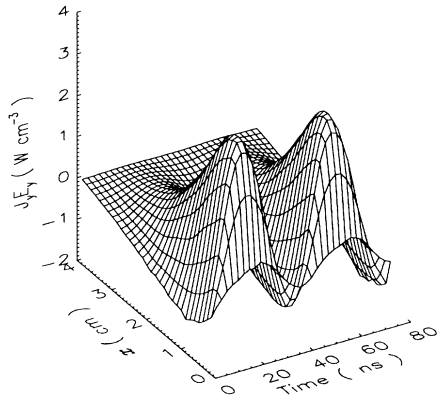

FIG. 5. The inductive electron heating, $J_y E_y$, as a function of time and position during a single rf cycle. The conditions are as in Fig. 4. The amplitudes of E_y and B_z that produce this heating are approximately 7 V cm^{-1} and 4 G, respectively, at $x = 0$.

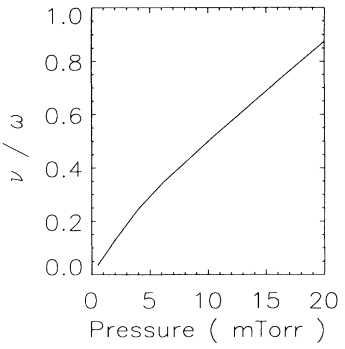

FIG. 6. The ratio ν/ω as a function of pressure, as calculated by the self-consistent simulation discussed in the text. In conjunction with Fig. 1, this figure shows that collisionless heating dominates for pressures less than 10 mTorr in argon.

place in hundreds, rather than thousands, of cycles. This was necessary because the large plasma density imposed a small integration time step. We held the boundary current density $\mathcal{J}_y$ constant at 600 A m^{-1} and varied the gas pressure in the range 0.5 to 20 mTorr. Figures 4 and 5 show something of the character of the converged solutions. Across the indicated range of pressure, the electron temperature varied from 10 eV to 4 eV, the plasma potential from 30 V to 20 V, and the plasma density from 10^{11} cm^{-3} to 10^{12} cm^{-3}. However, the parameter of present interest is ν/ω, which is shown as a function of pressure in Fig. 6. Comparison with Fig. 1 shows that the critical pressure for the onset of collisionless heating is $\sim$ 10 mTorr. At these electron temperatures, the role of the Ramsauer-Townsend effect [3] is small, so the threshold pressure for other gases is expected to be similar.

In summary, there is an important collisionless heating mechanism in H discharges which is closely analogous to the anomalous skin effect, a moderately famous phenomenon in metals [20]; the present study seems to be the first report of the anomalous skin effect as important in a classical plasma. These warm plasma effects require the Vlasov-Maxwell formalism for their analytical description, as we show above. A corollary of wide importance is that the complex wave equation (3) is not valid in the collisionless regime $\nu \lesssim \omega$, and therefore even sophisticated models that entail it [11] will not be universally valid. Warm plasma effects are properly included only when the thermal motion of electrons is closely coupled to the field solution, as in Eq. (8) or in the electromagnetic PIC simulation used in the present investigation.

This work was partially supported by EURATOM.

* Electronic address: (Internet) TURNERM@DCU.IE

[1] G. I. Babat, J. Inst. Electron. Eng. **94**, 27 (1947).
[2] V. A. Godyak, *Soviet Radio Frequency Discharge Research* (Delphic Associates, Inc., Falls Church, VA, 1986).
[3] V. A. Godyak and R. B. Piejak, Phys. Rev. Lett. **65**, 996 (1990).
[4] J. Hopwood, C. R. Guarnieri, S. J. Whitehair, and J. J. Cuomo, J. Vac. Sci. Technol. A **11**, 147 (1993).
[5] J. Hopwood, C. R. Guarnieri, S. J. Whitehair, and J. J. Cuomo, J. Vac. Sci. Technol. A **11**, 152 (1993).
[6] M. S. Barnes, J. C. Forster, and J. H. Keller, Appl. Phys. Lett. **62**, 2622 (1993).
[7] G. G. Lister and M. Cox, Plasma Sources Sci. Technol. **1**, 67 (1992).
[8] R. B. Piejak, V. A. Godyak, and B. M. Alexandrovich, Plasma Sources Sci. Technol. **1**, 179 (1992).
[9] E. M. Lifshitz and L. P. Pitaevskiĭ, *Physical Kinetics*, Course of Theoretical Physics Vol. 10 (Pergamon Press, Oxford, 1981).
[10] S. Ichimaru, *Basic Principles of Plasma Physics: A Statistical Approach*, Frontiers in Physics Vol. 41 (W. A. Benjamin, Inc., Reading, MA, 1973).
[11] P. L. G. Ventzek, R. J. Hoekstra, T. J. Sommerer, and M. J. Kushner, Appl. Phys. Lett. **63**, 605 (1993).
[12] C. K. Birdsall and A. B. Langdon, *Plasma Physics via Computer Simulation, The Adam Hilger Series on Plasma Physics* (Adam Hilger, Bristol, 1991).
[13] R. W. Hockney and J. W. Eastwood, *Computer Simulation Using Particles* (Adam Hilger, Bristol, 1988).
[14] C. K. Birdsall, IEEE Trans. Plasma Sci. **19**, 65 (1991).
[15] M. Hayashi, Technical Report No. IPPJ-AM-19, Nagoya Institute of Technology (unpublished).
[16] D. Rapp and P. Englander-Golden, J. Chem. Phys. **43**, 1464 (1965).
[17] K. Tachibana, Phy. Rev. A **34**, 1007 (1986).
[18] A. V. Phelps, J. Chem. Phys. Ref. Data **20**, 557 (1991).
[19] M. Surendra and D. B. Graves, Phys. Rev. Lett. **66**, 1469 (1991).
[20] The anomalous skin effect is important in pure metals at low temperature (liquid helium temperature) and at high frequency (microwave or radio frequency). These of course are so-called quantum plasmas, not classical plasmas. There are discussions in [9,21,22] and no doubt elsewhere. In his third edition (the relevant passage was excised in later revisions) Kittel [22] showed by informal argument that in metals the anomalous skin depth is given essentially by Eq. (10) of the present paper with the electron thermal velocity replaced by the Fermi velocity. Other treatments with varying degrees of rigor [9,21] give results that differ by a numerical factor of order 1.
[21] R. G. Chambers, *Electrons in Metals and Semiconductors* (Chapman and Hall, London, 1990).
[22] C. Kittel, *Introduction to Solid State Physics* (Wiley, New York, 1967), 3rd ed.